Accurate Eikonal-Curvature Relation for Wave Fronts in Locally Anisotropic Reaction-Diffusion Systems

Hans Dierckx,[1] Olivier Bernus,[2] and Henri Verschelde[1]

[1]*Department of Physics and Astronomy, Ghent University, 9000 Gent, Belgium*

[2]*Institute of Membrane and Systems Biology, Faculty of Biological Sciences, Multidisciplinary Cardiovascular Research Centre, University of Leeds, Leeds LS2 9JT, United Kingdom*

(Received 2 December 2010; revised manuscript received 23 June 2011)

The dependency of wave velocity in reaction-diffusion (RD) systems on the local front curvature determines not only the stability of wave propagation, but also the fundamental properties of other spatial configurations such as vortices. This Letter gives the first derivation of a covariant eikonal-curvature relation applicable to general RD systems with spatially varying anisotropic diffusion properties, such as cardiac tissue. The theoretical prediction that waves which seem planar can nevertheless possess a nonvanishing geometrical curvature induced by local anisotropy is confirmed by numerical simulations, which reveal deviations up to 20% from the nominal plane wave speed.

DOI: PACS numbers: 87.19.Hh, 05.45.−a, 87.10.−e

Reaction-diffusion (RD) equations govern a wide range of biological, physical, and chemical systems. A highly important emergent phenomenon is wave propagation, which is found in many RD systems such as flame-front propagation [1], waves in the Belousov-Zhabotinsky reaction [2], chemotactic signaling during morphogenesis of a social amoeba [3], waves of intracellular calcium [4], and electrical signaling in neuronal tissue [5]. The waves of excitation in cardiac tissue that initiate cardiac contraction are also being intensively studied, as abnormal wave propagation in the heart may lead to the formation of vortices and results in dangerous cardiac arrhythmias [6,7]. The key parameter that characterizes a propagating wave is its velocity; it turns out that the velocity of wave propagation in RD systems is affected by several factors, the curvature of the wave front being one of the most important. The dependency of the wave velocity on front curvature, i.e., the eikonal-curvature relation, was found in many systems [4,8–10], and it was also shown to be essential to the stability of the wave front and properties of vortices in the particular RD system. The simplest eikonal-curvature relation is given by the following linear relationship [8,9]:

$$c(k) = c_0 - \gamma k, \tag{1}$$

with c_0 the speed of a traveling plane wave in the given medium and γ a medium-dependent constant close to the scalar diffusivity of the isotropic medium [8,11]. Although stability analysis of Eq. (1) ensures stable propagating waves for positive γ, stability in critical media where γ lies close to zero is not guaranteed [12]. Remarkably, even when $\gamma > 0$, the linearized equation (1) exhibits no stable stationary solutions, although biological pattern formation is commonly modeled as a RD system, for which Eq. (1) can be derived. Another relevant RD system that conflicts with Eq. (1) is cardiac tissue, in which the propagation velocities of cardiac depolarization waves have been demonstrated to possess a ratio of (4:2:1) in orthogonal directions [13]. An earlier attempt to derive Eq. (1) in anisotropic media led to a complicated vectorial expression without a clear geometric interpretation [14].

Fortunately, the mathematical treatment of local anisotropy is greatly simplified when the curved-space formalism introduced in [15] is adopted. This formalism will not only allow us to generalize Eq. (1) to homogeneous excitable media of an arbitrary anisotropy type, but it also simplifies calculations such that the quadratic curvature corrections to the wave speed can be calculated for the first time. Our mathematical derivation provides an alternative and a generalization to Keener's seminal proof for the isotropic case, which relies on a boundary layer approximation and is thus restricted to the limit of steep wave fronts [9]. Here, Kuramoto's approach [8] is elaborated in a Riemannian context and pursued to higher order in curvature.

To start the derivation, the set of coupled reaction-diffusion equations (RDE) is written in terms of a column matrix $\mathbf{u}$ of state variables $u^{(m)}$, with the summation convention for repeated spatial indices,

$$\partial_t \mathbf{u}(\vec{r}, t) = \partial_i (D^{ij}(\vec{r}) \partial_j \mathbf{P}\mathbf{u}(\vec{r}, t)) + \mathbf{F}(\mathbf{u}(\vec{r}, t)). \tag{2}$$

Local anisotropy of the medium is embodied by the spatially varying diffusion tensor $D^{ij}(\vec{r})$. The constant projection matrix $\mathbf{P}$ selects only those state variables which diffuse into the medium. Inspired by studies on scroll wave filaments in excitable media, functional anisotropy will be handled by introducing the metric tensor [15,16]:

$$g_{ij} = D_0 (\mathbf{D}^{-1})_{ij}, \qquad g^{ij} = D_0^{-1} D^{ij}. \tag{3}$$

After denoting $D_0 \mathbf{P} = \hat{\mathbf{P}}$, we may recast the diffusion term in RDE (2) into $\hat{\mathbf{P}} \partial_i (g^{ij} \partial_j \mathbf{u})$. For homogenous media, the

determinant g of the metric in Cartesian coordinates is constant; long-wavelength deviations from homogeneity can be treated in perturbation theory [17]. Under such a condition, the diffusion term is proven to be equal to a covariant Laplacian [15]:

$$\partial_i(D^{ij}\partial_j \mathbf{P}\mathbf{u}) = g^{-1/2}\partial_i(g^{1/2}g^{ij}\partial_j \hat{\mathbf{P}}\mathbf{u}). \tag{4}$$

Subsequent calculations will greatly simplify if spatial Gaussian normal coordinates [18] are chosen, as depicted in Fig. 1; the time coordinate will be denoted τ. Defining the instantaneous wave front Σ as the hypersurface where a state variable $u^{(s)}$ crosses a threshold value $u_c^{(s)}$, it may be arbitrarily parametrized spatially as $X^i(\sigma^A), A \in \{1, \ldots, d-1\}$, in a RD medium with d dimensions. Points near Σ are represented by

$$x^i(\rho, \sigma^A, \tau) = X^i(\sigma^A, \tau) + \rho n^i(\sigma^A, \tau), \tag{5}$$

with $\vec{n}$ the local unit vector perpendicular to Σ and directed in the sense of wave propagation. This procedure reduces the metric tensor to

$$\mathbf{g}(\rho, \sigma^A, \tau) = \begin{pmatrix} 1 & 0\,0 \\ (0\,0)^T & \mathbf{h}(\rho, \sigma^A, \tau) \end{pmatrix}, \tag{6}$$

with $h_{AB} = e^i_A g_{ij} e^j_B$ the components of the metric that are induced on the wave front surface by the Riemannian background geometry. The change of coordinates gives rise to an associated biorthonormal reference triad $\vec{e}_\mu = \partial_\mu \vec{x}$, $\vec{e}^\mu = \vec{\nabla}\rho^\mu$, $(\mu \in \{\rho, \sigma^1, \sigma^2\})$ that satisfies $\vec{e}^\mu \cdot \vec{e}_\nu = \delta^\mu_\nu$. In terms of that triad, the wave front's geometric curvature with respect to the ambient RD medium is determined by the extrinsic curvature tensor $\mathbf{K}$ [18]:

$$K_A{}^B = \vec{e}^B \cdot \mathcal{D}_A \vec{e}_\rho = \Gamma^B_{A\rho}, \tag{7}$$

with Γ the metric connection and $\mathcal{D}_A$ a covariant derivative. Note that for $\rho \neq 0$, the tensor $\mathbf{K}$ refers to the local extrinsic curvature of surfaces at a fixed distance from the wave front. In definition (7), the sign of $K_A{}^B$ is taken such that convex fronts have positive curvature, in accordance with the chosen sign in Eq. (1). The trace of the extrinsic curvature tensor, denoted

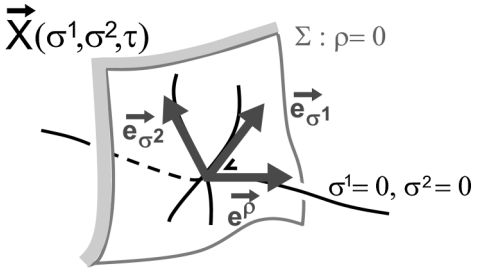

FIG. 1. Gaussian normal coordinates near the wave front.

$$K = \mathrm{Tr}(\mathbf{K}) = h^{AB}K_{AB} = \Gamma^A_{A\rho} = h^{-1/2}\partial_\rho h^{1/2}, \tag{8}$$

is the unique geometric invariant with dimension of inverse length that could replace k in Eq. (1); we will demonstrate shortly that this is indeed the case. Since the spatial extent over which the Gaussian normal coordinates can be consistently defined is limited by the front's local radius of curvature $\|\mathbf{K}\|_2^{-1}$, we introduce the dimensionless expansion parameter $\lambda = a\|\mathbf{K}\|_2$ for bookkeeping the sustained extrinsic curvature, with a the typical wave front thickness. Importantly, the geometrical expansion in λ distinguishes our approach from singular perturbation theory [9], and allows us to identify the higher order curvature corrections. Another source of curvature is the spatial variations in the diffusion tensor $\mathbf{D}$. Because of equivalence (3), the local anisotropy acts as an intrinsic curvature of the ambient space, which is fully captured by the Ricci curvature tensor $R_{\mu\nu}$ in three spatial dimensions [18]. Of special interest to wave front propagation is the $R_{\rho\rho}$ component, quantifying the relative acceleration of the geodesics perpendicular to the front surface. With Eq. (7) follows that

$$R_{\rho\rho} = R^A{}_{\rho A\rho} = -\partial_\rho K - \mathrm{Tr}(\mathbf{K}^2), \tag{9}$$

such that $R_{\rho\rho}$ can be considered $\mathcal{O}(\lambda^2)$ in what follows.

Knowing how both intrinsic and extrinsic curvature effects are bound by the parameter λ, we can now write down a gradient expansion series. Herein, the true solution $\mathbf{u}$ is approximated by the traveling wave profile $\mathbf{u}_0$ that satisfies RDE (2) in one spatial dimension:

$$\mathbf{u}(\rho, \sigma^A, \tau) = \mathbf{u}_0(\rho) + \tilde{\mathbf{u}}(\mathbf{K}(\rho, \sigma^A, \tau), \sigma^A, \rho, \tau). \tag{10}$$

Remark that in lowest order, the correction $\tilde{\mathbf{u}}$ will only depend on the wave front coordinates σ^A through the curvature $\mathbf{K}$. Because of translational symmetry of the RDE in an isotropic medium, this decomposition is *a priori* only fixed up to a term proportional to $\psi = \partial_\rho \mathbf{u}_0$. Therefore, we additionally impose that the correction $\tilde{\mathbf{u}}$ should be orthogonal to the unique zero mode $\mathbf{Y}$ of the adjoint operator $\hat{\mathbf{L}}^\dagger = D_0\mathbf{P}^T\partial_\rho^2 - c_0\partial_\rho + (\mathbf{F}'(\mathbf{u}_0))^T$. With bracket notation to indicate integration over ρ and summation over all state variables, the gauge condition that guarantees that $\tilde{\mathbf{u}} = \mathcal{O}(\lambda)$ can be written $\langle \mathbf{Y}|\tilde{\mathbf{u}}\rangle = 0$. Inserting Eqs. (4), (5), and (10) into RDE (2) then yields

$$\begin{aligned}
\partial_t \mathbf{u} &= \partial_\tau \tilde{\mathbf{u}} - (\vec{e}_\rho \cdot \dot{\vec{X}})(\partial_\rho \mathbf{u}_0 + \partial_\rho \tilde{\mathbf{u}} \\
&\quad + \partial_\rho K \partial_K \tilde{\mathbf{u}}) + \mathcal{O}(\lambda^3), \\
\partial_i(D^{ij}\partial_j \mathbf{P}\mathbf{u}) &= \Gamma^A_{A\rho}\hat{\mathbf{P}}\partial_\rho(\mathbf{u}_0 + \tilde{\mathbf{u}}) + \hat{\mathbf{P}}\partial_\rho^2(\mathbf{u}_0 + \tilde{\mathbf{u}}) \\
&\quad + 2\partial_\rho K\hat{\mathbf{P}}\partial_\rho(\partial_K \tilde{\mathbf{u}}) + \mathcal{O}(\lambda^3), \\
\mathbf{F}(\mathbf{u}) &= \mathbf{F}(\mathbf{u}_0) + \mathbf{F}'(\mathbf{u}_0)\tilde{\mathbf{u}} \\
&\quad + \tfrac{1}{2}\tilde{\mathbf{u}}\mathbf{F}''(\mathbf{u}_0)\tilde{\mathbf{u}} + \mathcal{O}(\lambda^3).
\end{aligned} \tag{11}$$

2

Using these relations along with $\vec{e}^{\rho} \cdot \dot{\vec{X}} = c$ and Eq. (8), the RDE transforms into an evolution equation for $\tilde{\mathbf{u}}$:

$$(\partial_\tau - \hat{\mathbf{L}})\tilde{\mathbf{u}} = (c - c_0)(\partial_\rho \mathbf{u}_0 + \partial_\rho \tilde{\mathbf{u}} + \partial_\rho K \partial_K \tilde{\mathbf{u}}) + K\hat{\mathbf{P}}\partial_\rho(\mathbf{u}_0 + \tilde{\mathbf{u}}) + 2\partial_\rho K \hat{\mathbf{P}}\partial_K \tilde{\mathbf{u}} + \tfrac{1}{2}\tilde{\mathbf{u}}\mathbf{F}''(\mathbf{u}_0)\tilde{\mathbf{u}} + \mathcal{O}(\lambda^3). \quad (12)$$

After $\langle \mathbf{Y}|$ has been normalized such that $\langle \mathbf{Y}|\psi\rangle = 1$, relation (12) can be projected onto this mode. With

$$\gamma = \langle \mathbf{Y}|\hat{\mathbf{P}}|\psi\rangle, \quad (13)$$

we obtain following eikonal-curvature relation that holds for RD media with generic local anisotropy:

$$c = c_0 - \gamma K + \mathcal{O}(\lambda^2). \quad (14)$$

Importantly, the suitable modification to the wave front curvature k that was sought for in [14] is recognized here as the trace of the extrinsic curvature tensor defined by Eq. (7). Alternatively, Eq. (14) could have been obtained directly by writing Eq. (1) in a covariant way.

To track higher order curvature effects, the perturbation $\tilde{\mathbf{u}}$ to the wave profile needs further specification. As we intend to develop a theory that is local in space and time, an estimate to $\tilde{\mathbf{u}}$ using Eq. (12) can be easily made in the quasistationary regime, i.e., if $\tilde{\mathbf{u}}$ accommodates nearly instantaneously to its stationary state after a change in the extrinsic curvature. Taking into account the first-order result (14), the perturbative correction is then found from Eq. (12) as the solution to $\hat{\mathbf{L}}|\tilde{\mathbf{u}}\rangle = (\gamma\mathbf{I} - \hat{\mathbf{P}})|\psi\rangle K + \mathcal{O}(\lambda^2)$. Since the right-hand side of this equation has no component along the null space of $\hat{\mathbf{L}}$, it follows that $|\tilde{\mathbf{u}}\rangle = K|\mathbf{u}_1\rangle + \mathcal{O}(\lambda^2)$, where $|\mathbf{u}_1\rangle = \hat{\mathbf{L}}^{-1}(\gamma\mathbf{I} - \hat{\mathbf{P}})|\psi\rangle$. Plugging this result into Eq. (12) and projecting onto the zero mode $\langle \mathbf{Y}|$ delivers

$$c = c_0 - \gamma K - \eta\partial_\rho K - \zeta K^2 + \mathcal{O}(\lambda^3), \quad (15)$$

with two novel coefficients that arise as overlap integrals:

$$\zeta = \langle \mathbf{Y}|(\hat{\mathbf{P}} - \gamma\mathbf{I})\partial_\rho|\mathbf{u}_1\rangle - \tfrac{1}{2}\langle \mathbf{Y} \mid \mathbf{u}_1\mathbf{F}''(\mathbf{u}_0)\mathbf{u}_1\rangle,$$
$$\eta = \langle \mathbf{Y}|\rho\hat{\mathbf{P}}|\psi\rangle + 2\langle \mathbf{Y}|\hat{\mathbf{P}}|\mathbf{u}_1\rangle. \quad (16)$$

Equations (14)–(16) are the main result in this work, as they generalize and extend previous descriptions of wave propagation in RD media obtained for specific approximations [8,9,11,14,19]. In general geometrical terms, Eq. (15) demonstrates that the intrinsic curvature of the RD medium does not directly alter the wave velocity; local anisotropy only affects wave dynamics by changing local length scales and through the extrinsic curvature. The absence of a $R^2{}_{323}$ term could have been expected, since this quantity probes the internal structure of the front, along which no physical diffusion takes place.

Another merit of Eq. (15) is the quantification of two previously inaccessible effects: a correction $(\partial_\rho K)$ due to the finite width of the wave front, and a term (K^2) that captures how wave propagation is altered by curvature-induced modification of the wave profile. A first corollary of the second order curvature corrections is that a nonlinear $c(K)$ relation could explain how patterns of finite size may emerge in an otherwise homogenous RD medium, thereby allowing richer dynamics in pattern formation. Second, linear stability analysis shows that small ripples with wave vector $p\vec{u}$ on the wave front surface grow with a rate $\Omega = -p^2\gamma_{\text{eff}}(K)$, where

$$\gamma_{\text{eff}}(K) = \gamma + 2\zeta K + 2\eta K_{AB}u^A u^B + \mathcal{O}(\lambda^2). \quad (17)$$

Hence, wave fronts are dynamically stable only if $\gamma_{\text{eff}} > 0$. This observation suggests to enlarge Kuramoto's notion of surface tension γ [8] to the effective dynamical surface tension $\gamma_{\text{eff}}(K)$ defined by Eq. (17). Consequently, the stability of systems with $\gamma \approx 0$ depends on their local curvature. This effect was seen already in the numerical simulation of RD systems with high inhibitor diffusion [12].

To highlight the importance of the curved-space viewpoint, we next provide an example of wave fronts that appear flat to a laboratory observer. The parameters (σ^1, σ^2) within a seemingly planar wave front surface can be chosen linear in the Cartesian coordinates, whence the $\vec{e}_A$ are constant. As such, those waves would bear a constant induced metric $H_{AB} = e^i_A \delta_{ij} e^j_B$ if the ambient space had been Euclidean. When anisotropy is taken into account, however, a spatially varying metric $h_{AB} = e^i_A g_{ij} e^j_B$ is seen to be induced, delivering nonvanishing curvature terms in Eq. (16) through Eq. (8). Therefore, waves that appear planar from the laboratory viewpoint do not necessarily travel at the nominal plane wave speed c_0, even when the traveled distance is measured using the metric (3). This prediction is confirmed below by numerical simulation.

Three steps of numerical validation of Eqs. (15) and (16) were performed using Barkley's model with equations as in [20], which is often used as a paradigm for RD systems, as it is computationally efficient and exhibits the key features of an excitable medium [21]. First, theoretical predictions for the coefficients γ, ζ, η were explicitly evaluated as overlap integrals (13) and (16) of the adjoint zero mode $\langle \mathbf{Y}|$, which had been obtained as the stationary solution to $\partial_t \mathbf{u} = \hat{\mathbf{L}}^\dagger \mathbf{u}$, similar to [22]. Second, these coefficients were estimated from the dynamics of inwardly traveling spherical wave fronts, which were simulated using finite differences in the radial coordinate r. Repeating the simulations for a d-dimensional isotropic RD medium, with $d \in \{2, 3, 4\}$ allowed to separate all contributions by linear regression, as the waves have $K = -(d-1)/r$. Note, however, that the wave front's position is found in practice by applying a threshold to $\mathbf{u}$, not $\mathbf{u}_0$, which shifts the measured coefficient of $\partial_\rho K$ from η to $\eta' = \eta - c_0 u_1^{(s)}(0)/\psi^{(s)}(0)$. Figure 2 displays the values of γ, ζ, η'

3

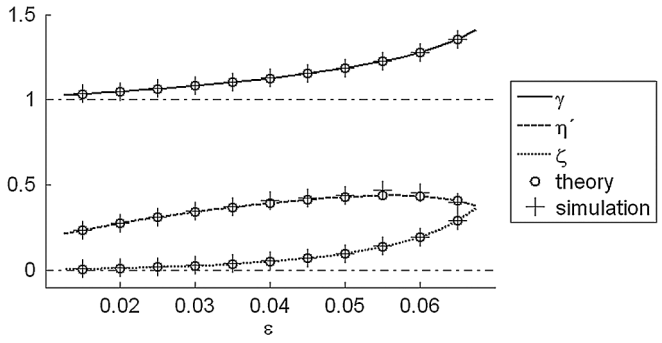

FIG. 2. Coefficients in Eq. (13) for the model [20].

obtained from forward numerical simulation and theory, for varying model parameter ϵ. The quantitative comparison demonstrates an excellent agreement between predicted and measured values with average relative errors of 0.2%, 2.2%, and 5.4% in the predictions for γ, η', and ζ, even though ζ and η' are composed of 2 and 3 terms of comparable magnitude.

In a third numerical simulation, traveling waves were studied in a model geometry for the cardiac wall exhibiting transmural myofiber rotation [23]. In terms of Cartesian coordinates (x, y, z), the medium with so-called rotational anisotropy is considered invariant in X and Y directions, and a prototypical fiber with diffusion tensor $\mathbf{D} = \mathrm{diag}(9, 1, 1)$ rotates at a pitch p around the Z axis with increasing z; the angle θ between the fiber direction and X direction is thus equal to pz. At the start of each simulation, a plane wave was initiated containing the Y direction and enclosing a chosen angle ψ with the X direction. After a short transient time, wave front velocity was recorded, using Eq. (3) as a measure for the traveled distance. The numerical result is presented in Fig. 3 in terms of the transmural position $\theta = pz$, together with the prediction of Eq. (15) up to zeroth, first, and second order in curvature. Substantial curvature effects were observed, which caused deviations up to over 20% of the wave speed. Notwithstanding the magnitude of this

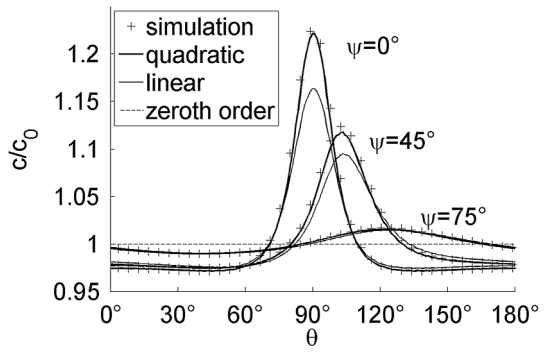

FIG. 3. Waves that appear planar to the laboratory observer, in a medium with constant fiber rotation rate p: local normal velocity vs transmural coordinate $\theta = pz$.

effect, the velocities predicted by Eqs. (13)–(15) were found to match the simulated values within 0.5%, without any free parameters present.

Our results show that the smallest curvature effects are found for nearly transmural wave propagation (i.e., along the Z axis or $\psi \to 90°$), which typically occur in the heart's natural activation sequence. On the other hand, for intramural wave propagation ($\psi \to 0°$), which may occur during abnormal activation and arrhythmias [6], considerably larger curvature corrections are found in the computational example (Fig. 3), consistent with Eq. (13). In this case, the linear term does not longer suffice to correctly predict wave front velocity.

In summary, we have taken a curved-space viewpoint on local anisotropy of RD systems to establish an accurate velocity-curvature relation for activation waves in its simplest form. Although our approach was tailored to describe wave phenomena in anisotropic cardiac tissue with increased accuracy, our findings can be readily applied to wave propagation problems in a wide variety of RD systems, including bistable and excitable media.

H. D. thanks the FWO–Flanders Research Foundation for personal funding and computational infrastructure. The authors are grateful to Dr. A. V. Panfilov for suggestions on improving the manuscript.

[1] G. I. Sivashinsky, Acta Astronaut. **4**, 1177 (1977).
[2] A. N. Zaikin and A. M. Zhabotinsky, Nature (London) **225**, 535 (1970).
[3] F. Siegert and C. J. Weijer, Proc. Natl. Acad. Sci. U.S.A. **89**, 6433 (1992).
[4] J. Lechleiter, S. Girard, E. Peraltal, and D. Clapham, Science **252**, 123 (1991).
[5] A. L. Hodgkin and A. F. Huxley, J. Physiol. **117**, 500 (1952).
[6] *Cardiac Electrophysiology: From Cell to Bedside* edited by D. P. Zipes and J. Jalife (Saunders, Philadelphia, 1995), 2nd ed.
[7] C. Cabo, A. M. Pertsov, J. M. Davidenko, and J. Jalife, Biophys. J. **70**, 1105 (1996).
[8] Y. Kuramoto, Prog. Theor. Phys. **63**, 1885 (1980).
[9] J. P. Keener, SIAM J. Appl. Math. **46**, 1039 (1986).
[10] P. Colli-Franzone, L. Guerri, and S. Tentoni, J. Math. Biol. **28**, 121 (1990).
[11] A. S. Mikhailov, V. A. Davydov, and V. S. Zykov, Physica (Amsterdam) **70D**, 1 (1994).
[12] V. S. Zykov, A. S. Mikhailov, and S. C. Müller, Phys. Rev. Lett. **81**, 2811 (1998).
[13] B. J. Caldwell, M. L. Trew, G. B. Sands, D. A. Hooks, I. J. LeGrice, and B. H. Smaill, Circ. Arrhythm. Electrophysiol. **2**, 433 (2009).
[14] J. P. Keener, J. Math. Biol. **29**, 629 (1991).
[15] H. Verschelde, H. Dierckx, and O. Bernus, Phys. Rev. Lett. **99**, 168104 (2007).
[16] M. Wellner, O. M. Berenfeld, J. Jalife, and A. M. Pertsov, Proc. Natl. Acad. Sci. U.S.A. **99**, 8015 (2002).

4

[17] H. Dierckx, O. Bernus, and H. Verschelde, Physica (Amsterdam) **238D**, 941 (2009).
[18] C. W. Misner, K. S. Thorne, and J. A. Wheeler, *Gravitation* (W. H. Freeman and Co., San Francisco, 1973).
[19] R. J. Young and A. V. Panfilov, Proc. Natl. Acad. Sci. U.S.A. **107**, 15 063 (2010).
[20] $F^{(1)} = \epsilon^{-1} u^{(1)}(1 - u^{(1)})(u^{(1)} - (u^{(2)} + b)/a)$, $F^{(2)} = u^{(1)} - u^{(2)}$. Parameters $a = 0.75$, $b = 0.02$, $\epsilon = 0.04$.
[21] D. Barkley, Physica (Amsterdam) **49D**, 61 (1991).
[22] I. V. Biktasheva, A. V. Holden, and V. N. Biktashev, Int. J. Bifurcation Chaos Appl. Sci. Eng. **16**, 1547 (2006).
[23] F. H. Fenton and A. Karma, Chaos **8**, 20 (1998).

5